HEPATOBILIARY

Can modified LI-RADS increase the sensitivity of LI-RADS v2018 for the diagnosis of 10–19 mm hepatocellular carcinoma on gadoxetic acid-enhanced MRI?

Sidong Xie[1] · Yao Zhang[1] · Jingbiao Chen[1] · Ting Jiang[1] · Weimin Liu[1] · Dailin Rong[1] · Lin Sun[1] · Linqi Zhang[1] ·
Bingjun He[1] · Jin Wang[1]

Abstract

Purpose To evaluate whether the Liver Imaging Reporting and Data System (LI-RADS) v2018 LR-5 criteria can be modified to increase sensitivity without reducing specificity for diagnosing 10–19 mm hepatocellular carcinoma (HCC) on gadoxetic acid-enhanced magnetic resonance imaging (MRI).

Methods A total of 133 high-risk consecutive patients with 174 small observations (10–19 mm) detected on gadoxetic acid-enhanced MRI were retrospectively studied. LI-RADS MRI major features (MFs) and ancillary features (AFs) were reviewed by two independent radiologists in consensus. Observations were categorized using LI-RADS v2018 MFs. Independently significant AFs were identified through logistic regression analysis. Upgraded LR-5 criteria were developed by combining independently significant AFs with MFs of LR-3 or LR-4 v2018. The sensitivity and specificity of the new diagnostic criteria were compared with those of LR-5 v2018 using McNemar's test.

Results Three of the AFs favoring malignancy [mild–moderate T2 hyperintensity, transitional phase (TP) hypointensity and fat in mass] were independently significant features for diagnosing 10–19 mm HCC. The upgraded LR-5 criteria (mLI-RADS VII: LR-4 + mild–moderate T2 hyperintensity/TP hypointensity or LR-3 + fat in mass) yielded a significantly greater sensitivity than that of the LR-5 v2018 criteria (70.4% vs 55.1%; $p < 0.001$), whereas the specificity was not significantly different (94.7% vs 98.7%, $p = 0.250$).

Conclusions Independently significant AFs may be used to upgrade an observation from LR-3/LR-4 to LR-5, which can improve the sensitivity without impairing the specificity for diagnosing 10–19 mm HCC on gadoxetic acid-enhanced MRI.

Sidong Xie and Yao Zhang have contributed equally to this work.

✉ Jin Wang
 wangjin3@mail.sysu.edu.cn

[1] Department of Radiology, The Third Affiliated Hospital,
 Sun Yat-sen University (SYSU), No 600, Tianhe Road,
 Guangzhou 510630, Guangdong, People's Republic of China

Graphical abstract
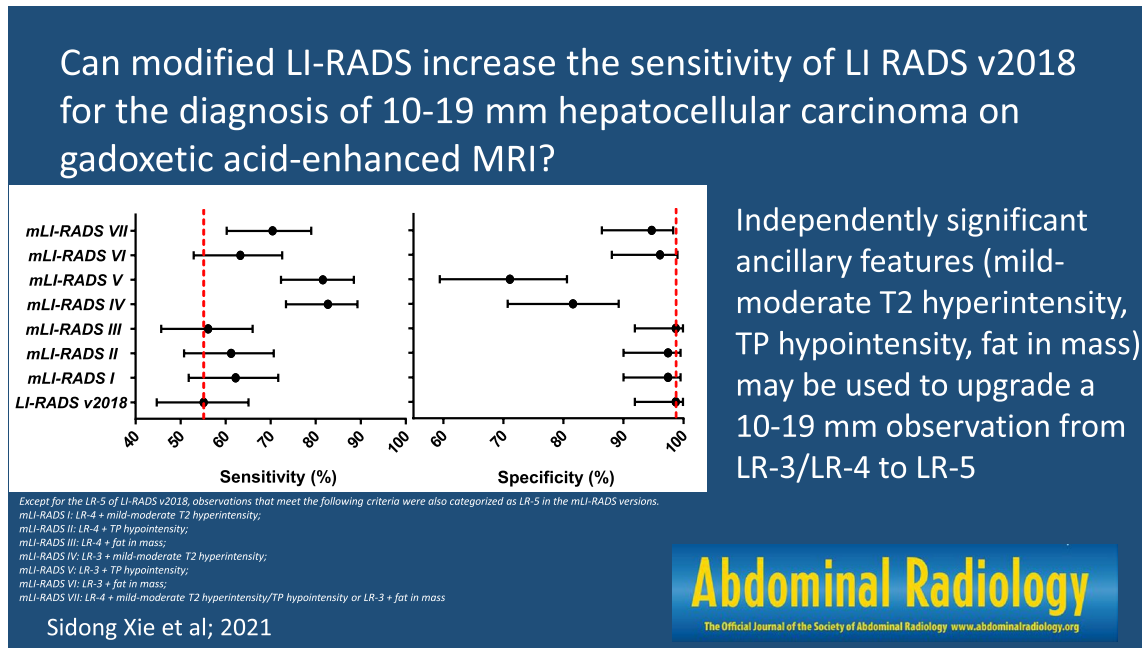
Keywords Liver neoplasms · Diagnosis · Sensitivity and specificity · Magnetic resonance imaging · Gadoxetic acid

Introduction

Hepatocellular carcinoma (HCC) is the sixth most common cancer in the world and the fourth leading cause of cancer-related death worldwide [1]. The early detection and management of small (< 20 mm) HCCs can prolong patient survival [2]. Unlike other malignancies that require histological diagnosis, HCC can be diagnosed noninvasively according to imaging-based criteria without confirmatory pathology [3–5].

The Liver Imaging Reporting and Data System (LI-RADS) is widely accepted as a good scheme for interpreting and reporting imaging features of liver observations in patients at high risk for HCC [6–8]. LI-RADS version 2018 (hereafter LI-RADS v2018) represents the fourth update of this HCC imaging system since its first release in 2011. In LI-RADS v2018, a 10–19 mm observation with nonrim arterial-phase hyperenhancement (APHE) plus nonperipheral "washout" or threshold growth is now categorized as LR-5. The updated LI-RADS v2018 have been integrated into the 2018 American Association for the Study of Liver Disease (AASLD) guidance and is expected to improve the diagnosis of HCC. However, few studies have reported the diagnostic performance of LI-RADS v2018 for 10–19 mm HCC lesions on gadoxetic acid-enhanced magnetic resonance imaging (MRI) [9].

In clinical practice, small hepatic nodules (< 20 mm) often pose a diagnostic challenge due to their atypical imaging feature on either contrast-enhanced computed tomography (CECT) or MRI. Prior studies involving small nodules (< 20 mm) have demonstrated higher sensitivity for small HCC lesions on gadoxetic acid-enhanced MRI than those observed on multiphasic CT or extracellular contrast-enhanced MRI [10–12] at the expense of reduced specificity. The hypointensity on TP is not a real washout when using Gd-EOB-DTPA, since it is a combination of a true vascular washout and an increased enhancement of the background liver [13–16]. Therefore, in the latest versions of AASLD guidance, the European Association for the Study of the Liver (EASL) and LI-RADS v2018, the nonperipheral washout appearance on gadoxetic acid-enhanced MRI can be depicted only in the portal venous phase (PVP). On the other hand, that results in reduced diagnostic sensitivity for HCC (66.3–77.9%) [15, 17, 18]. Furthermore, some ancillary features (AFs), such as hepatobiliary phase (HBP) hypointensity and restricted diffusion, are strong indicators of malignancy and play important roles in the diagnosis of HCC [19]. However, in the current LI-RADS version, the diagnosis of HCC is primarily based on major features (MFs), and the use of AFs is optional. In addition, using AFs, an observation can be upgraded by one category up to LR-4 but not to LR-5. Therefore, the weight of AFs in the diagnosis of HCC may be somehow overlooked.

Therefore, the purpose of this study was to evaluate the diagnostic performance of LI-RADS v2018 for 10–19 mm HCC and to explore whether modifications to LI-RADS using AFs could further improve sensitivity without reducing specificity for HCC on gadoxetic acid-enhanced MRI.

Materials and methods

Patients

This retrospective study was approved by our institutional review board, and the requirement for written informed consent was waived. From June 2015 to April 2017, a total of 830 patients who underwent gadoxetic acid-enhanced 1.5-T or 3.0-T MRI examination for the evaluation of suspicious nodules at our center were included. The inclusion criteria were as follows: (a) age ≥ 18 years old; (b) high risk for HCC according to LI-RADS v2018 (cirrhosis or chronic hepatitis B viral infection); (c) observation size of 10–19 mm and ≤ 4 nodules observed in one patient using contrast-enhanced MRI with gadoxetate disodium; and (d) no previous treatment for hepatic lesions. The exclusion criteria were as follows: (a) no observations other than hepatic cysts on MRI; (b) congestive hepatopathies, such as hereditary hemorrhagic telangiectasia, Budd–Chiari syndrome, chronic portal vein occlusion, and cardiac congestion; and (c) an insufficient final diagnosis (e.g., histopathologic diagnosis more than 2 months after MRI examination, inconclusive histopathologic diagnosis, immediate local treatment or systemic therapy without pathologic diagnosis, and insufficient follow-up to determine size stability) or unsatisfactory image quality for analysis. The process of patient selection for the study cohort is shown in Fig. 1.

MRI examination

All patients were scanned in a supine position on a 1.5-T (Optima MR360, GE Healthcare) or a 3.0-T whole-body MRI scanner (Discovery MR750, GE Healthcare) with an eight-channel phased-array torso coil centered over the abdomen. Routine MRI sequences included T2-weighted, diffusion-weighted, in-and out-of-phase, unenhanced T1-weighted, dynamic, and HBP sequences using gadoxetate disodium (Primovist; Bayer Healthcare). The contrast agent was automatically administered intravenously using a power injection device (Spectris Solaris EP; MEDRAD) at a rate of 2.0 ml/s for a total dose of 0.025 mmol/kg body weight, followed by a 20-ml saline flash. The dual arterial phase (AP) was initiated 15–30 s after the contrast agent arrived at the pulmonary artery using bolus triggering. The dual PVP and transitional phase (TP) were acquired at 50–80 s and 3 min, respectively. HBP images were obtained 20 min after contrast agent injection. Imaging examinations were in compliance with LI-RADS technical requirements. Scanning parameters are listed in Supplementary Table 1.

MRI analysis and LI-RADS category assignment

All MRI scans were retrieved from the picture archiving and communication system (PACS) and reviewed by two abdominal radiologists [with 14 years (Sidong Xie) and 9 years (Jingbiao Chen) of experience in liver MRI]. Blinded to the reference standard, they independently evaluated the following imaging features defined in LI-RADS v2018 for every observation found on each patient's MRI examination [20]: MFs and AFs favoring malignancy, and AFs favoring benignity, targetoid features and tumor in vein (TIV). If an observation showed high signal intensity on T1-weighted imaging (T1WI) before the administration of gadoxetic acid, APHE was evaluated by subtracting arterial-phase images. Discrepancies were resolved by consensus. After scoring all the imaging features, the two radiologists assigned a LI-RADS category to each observation according to only the major imaging features of LI-RADS v2018. Subsequently, LI-RADS categorization were assigned using MFs and independent significant AFs in combination.

Reference standard

The final diagnoses of HCC and non-HCC malignancies were confirmed by histopathology (hepatectomy specimen or liver biopsy). An experienced histopathologist (Jianning Chen) blinded to all clinical data and MRI results reviewed the histological specimens and confirmed the histological diagnosis according to the World Health Organization classification system [21]. The benign lesions were confirmed by pathology or typical imaging features and stability on imaging for at least 2 years.

The presence or absence of liver cirrhosis was evaluated by the same pathologist according to the background liver adjacent to the tumor in patients who underwent surgical treatment. In patients who did not undergo surgery, the diagnosis of cirrhosis was determined by the two radiologists according to the morphological MRI features, including a nodular contour of the liver, segmental atrophy, and widened fissures or gallbladder fossa, regardless of varices, ascites, or splenomegaly [22].

Statistical analysis

Continuous data are summarized as the mean and standard deviation or median and range. Categorical data are summarized as counts and percentages. Per-observation estimates of the diagnostic performance for each MF and AF were calculated. Univariate and multivariate logistic
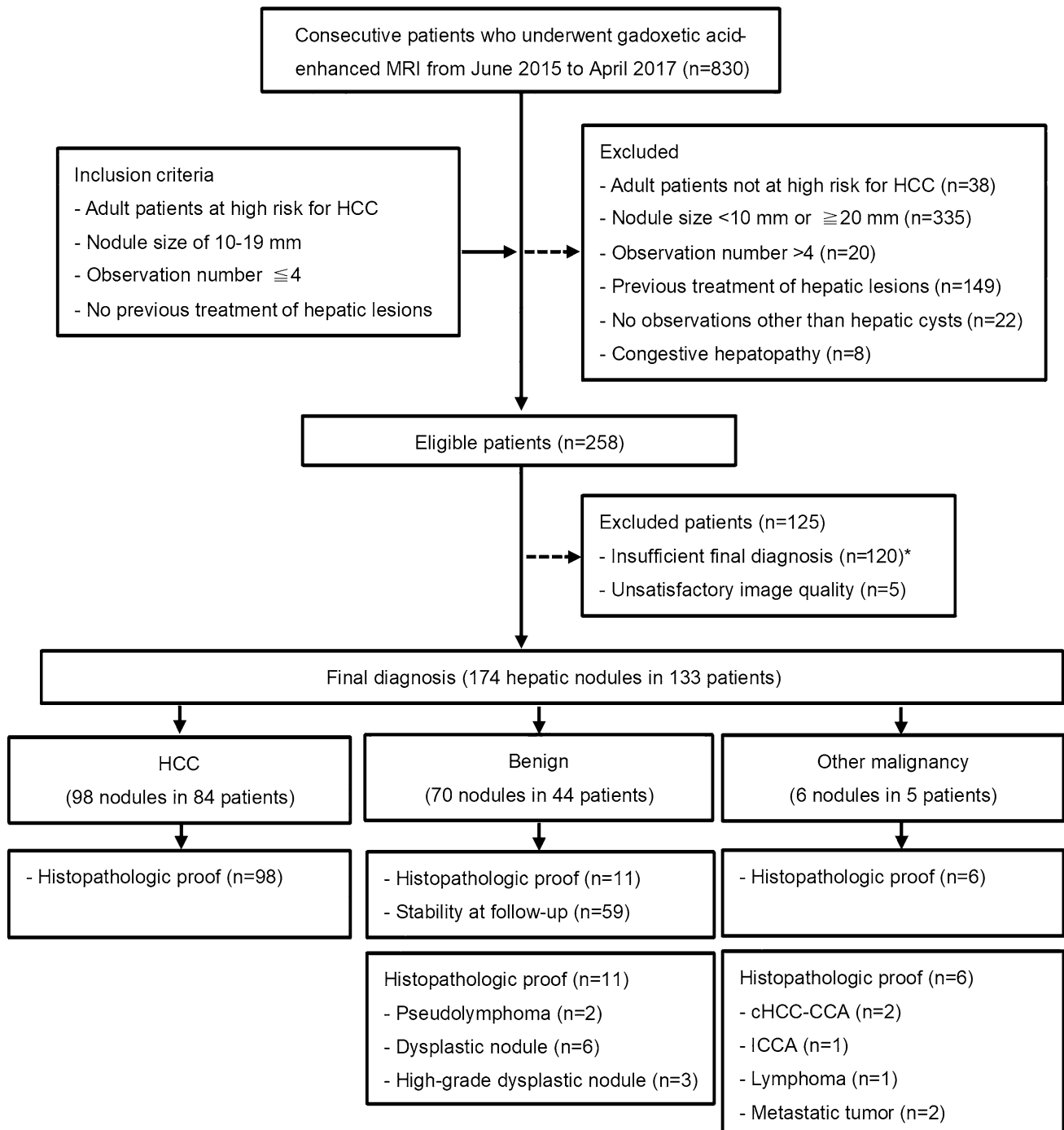
Fig. 1 Process of patient selection for the study cohort. *HCC* hepatocellular carcinoma, *MRI* magnetic resonance imaging, *cHCC-CCA* combined HCC-cholangiocarcinoma, *ICCA* intrahepatic cholangiocarcinoma. *Patients with an insufficient final diagnosis (*n* = 120) included patients with a histopathologic diagnosis more than 2 months after the MRI examination (*n* = 30), an inconclusive histopathologic diagnosis (*n* = 17), immediate local treatment or systemic therapy without a pathologic diagnosis (*n* = 50), and insufficient follow-up to determine size stability (*n* = 23)

regression analyses were performed to determine the independent predictors for HCC among the AFs according to LI-RADS v2018. Variables with a *p* value < 0.05 in the univariable analysis were entered into the multivariable analysis to identify independently significant AFs for HCC diagnosis. For the multivariable analysis, a stepwise backward elimination method was used. The sensitivity and specificity of different modified LI-RADS for HCC were

compared with those of LI-RADS v2018 using McNemar's test.

The kappa (κ) statistic was used to determine interobserver agreement for the LI-RADS features. The interpretation of κ values was as follows: poor, 0.00–0.20; fair, 0.21–0.40; moderate, 0.41–0.60; good, 0.61–0.80; and excellent, 0.81–1.00.

SPSS software version 22.0 (IBM) was used for all statistical analyses. $p < 0.05$ was considered statistically significant.

Results

Patients

A total of 133 patients (129 males and 4 females; median age 52.0 years) with 174 observations were finally included. The demographics and clinical and biological characteristics of the patients are summarized in Table 1. Of the 133 patients, 103 (77.4%) patients had a single observation, and 29 (21.8%) patients had more than one observation. Among the 133 patients, 128 (96.2%) patients had hepatitis B virus (HBV) infection, while 82 (61.7%) patients had liver cirrhosis. Regarding the liver function estimation, the majority of patients (85.0%) were Child–Pugh class A.

Final diagnoses

Among the 174 observations, 104 (59.8%) and 70 (40.2%) were malignant and benign lesions, respectively. A total of 115 (66.1%) observations were pathologically proven, including all HCC ($n = 98$) and non-HCC ($n = 6$) malignancies [i.e., combined HCC-cholangiocarcinoma (cHCC-CCA, $n = 2$), intrahepatic cholangiocarcinoma (ICCA, $n = 1$), lymphoma ($n = 1$), and metastasis ($n = 2$)], and 11 benign lesions [i.e., pseudo-lymphoma ($n = 2$), dysplastic nodule ($n = 6$) and high-grade dysplastic nodule ($n = 3$)]. The types of procedures performed for histopathologic confirmation of hepatic observations included surgical resection ($n = 48$), ablation after US-guided needle biopsy ($n = 64$), and liver transplantation ($n = 3$). The other benign lesions ($n = 59$) were confirmed by a composite of clinical and MRI follow-up, including 24 (40.7%) hemangiomas and 4 (6.8%) perfusion alterations based on typical imaging features by the two radiologists in consensus. The other 31 (52.5%) lesions were interpreted by the two radiologists as benign hepatocellular nodules based on imaging features and longitudinal stability.

Interobserver agreement of the MRI features

The interobserver agreement of MFs and AFs favoring malignancy of LI-RADS v2018 is shown in Supplementary

Table 1 Clinicopathologic characteristics of patients and lesions

Characteristic	Value
Patient ($n = 133$)	
Mean age (years)**	52.0 (44.0–59.0)
Sex*	
Male	129 (97.0)
Female	4 (3.0)
BMI**	23.8 (21.5–25.1)
Cirrhosis*	
Presence	82 (61.7)
Absence	51 (38.3)
Cause of liver disease*	
Hepatitis B virus	128 (96.2)
Hepatitis C virus	1 (0.8)
Hepatitis B and C virus	1 (0.8)
Alcoholic liver disease	3 (2.3)
No. of observations per patient*	
1	103 (77.4)
2	21 (15.8)
3	8 (6.0)
4	1 (0.8)
Child–Pugh Class*	
Class A	113 (85.0)
Class B	16 (12.0)
Class C	4 (3.0)
Total bilirubin (μmol/L)**	15.40 (12.00–24.00)
Tumor marker (ng/mL)**	
AFP	17.55 (3.68–91.14)
Lesion ($n = 174$)	
Mean size (mm)#	14.5 ± 2.9
Final diagnosis*	
HCC	98 (56.3)
Non-HCC malignancy	6 (3.5)
cHCC-CCA	2 (1.15)
ICCA	1 (0.6)
Lymphoma	1 (0.6)
Metastasis	2 (1.15)
Benign lesion	70 (40.2)
Standard reference of diagnosis*	
Pathologic diagnosis	115 (66.1)
Typical imaging features with size stability (2 years)	59 (33.9)

IQR interquartile range, *AFP* alpha fetoprotein, *cHCC-CCA* combined HCC-cholangiocarcinoma, *ICCA* intrahepatic cholangiocarcinoma

*Data are shown as n (%)

**Data are shown as the median (IQR)

#Data are continuous variables, reported as the mean ± standard deviation

Table 2. The agreement between the two observers for LI-RADS features was moderate to excellent, with κ values ranging from 0.66 to 1.00.

Independently significant AFs for diagnosing HCC

The univariate analysis demonstrated that AFs favoring malignancy (restricted diffusion, mild–moderate T2 hyperintensity, TP hypointensity, HBP hypointensity, US visibility, fat in mass and mosaic architecture) had significant value for predicting HCC ($p < 0.001$, < 0.001, < 0.001, < 0.001, < 0.001, 0.001, and 0.049, respectively; Table 2). According to the multivariate analysis, mild–moderate T2 hyperintensity [odds ratio (OR), 5.1; 95% confidence interval (CI), 2.1–12.7; $p < 0.001$], TP hypointensity (OR, 3.6; 95% CI, 1.1–11.8; $p = 0.032$) and fat in mass (OR, 3.3; 95% CI, 1.0–10.2; $p = 0.043$) were independently significant AFs for identifying 10–19 mm HCC (Table 2).

Based on the above results of the univariate and multivariate analyses, we developed a modified LI-RADS with the upgraded LR-5 criteria by combining LR-3/LR-4 v2018 classified by MFs alone, with these three independently significant AFs identified from the multivariable analysis. In different modified LI-RADS versions, except for the LR-5 observations as defined by LI-RADS v2018, observations that meet the following criteria were also categorized as

LR-5 in the mLI-RADS versions. The modified LI-RADS was as follows:

mLI-RADS I: LR-4 + mild–moderate T2 hyperintensity;
mLI-RADS II: LR-4 + TP hypointensity;
mLI-RADS III: LR-4 + fat in mass;
mLI-RADS IV: LR-3 + mild–moderate T2 hyperintensity;
mLI-RADS V: LR-3 + TP hypointensity;
mLI-RADS VI: LR-3 + fat in mass; and
mLI-RADS VII: LR-4 + mild–moderate T2 hyperintensity/TP hypointensity or LR-3 + fat in mass (Figs. 2, 3).

Diagnostic performance of LI-RADS v2018 and different LI-RADS versions

Distribution and interobserver agreement for conventional LI-RADS v2018 categories are shown in Supplementary Table 3. Using LI-RADS v2018, 18 (10.3%), 26 (14.9%), 58 (33.3%), 8 (4.6%), 55 (31.6%), and 9 (5.2%) observations were categorized as LR-1, LR-2, LR-3, LR-4, LR-5, and LR-M, respectively. No observations were categorized as LR-TIV. Among 174 observations, 0% (0/18) of LR-1, 0% (0/26) of LR-2, 56.9% (33/58) of LR-3, 87.5% (7/8) of LR-4, 98.2% (54/55) of LR-5, and 44.4% (4/9) of LR-M were HCCs in LI-RADS v2018. The number of HCC identified as LR-5 in LI-RADS v2018, mLI-RADS I, mLI-RADS II, mLI-RADS III, mLI-RADS IV, mLI-RADS V, mLI-RADS VI and mLI-RADS VII were 54/174, 61/174, 60/174,

Table 2 Logistic regression analyses of ancillary features favoring malignancy in LI-RADS v2018 for diagnosing 10–19 mm HCC

Parameter	Univariable analysis		Multivariable analysis	
	OR	p value	OR	p value
LI-RADS ancillary features (favoring HCC in particular)				
Nonenhancing "capsule"	1.6 (0.3–8.8)	0.606		
Nodule-in-nodule architecture	$1.3 \times 10E9$ (0.0–)	0.999		
Mosaic architecture	4.7 (1.0–21.8)	0.049	1.4 (0.2–8.1)	0.700
Blood products in mass	$1.3 \times 10E9$ (0.0–)	0.999		
Fat in mass	5.7 (2.1–15.6)	0.001	3.3 (1.0–10.2)	0.043
LI-RADS ancillary features (favoring malignancy in general)				
Restricted diffusion	6.9 (2.9–16.4)	<0.001	1.1 (0.3–3.6)	0.865
Mild–moderate T2 hyperintensity	8.6 (4.3–17.5)	<0.001	5.1 (2.1–12.7)	<0.001
Transitional-phase hypointensity	10.4 (4.6–23.7)	<0.001	3.6 (1.1–11.8)	0.032
Hepatobiliary-phase hypointensity	15.5 (4.5–53.9)	<0.001	2.9 (0.5–17.0)	0.238
Coronal enhancement	$1.3 \times 10E9$ (0.0–)	0.999		
US visibility as discrete nodule	3.1 (1.6–5.7)	<0.001	1.9 (0.9–4.2)	0.097
Subthreshold growth	0.8 (0.2–3.2)	0.713		
Fat sparing	0.6 (0.2–2.3)	0.465		
Iron sparing	1.3 (0.6–2.7)	0.457		

Data of sensitivity and specificity are shown as the number of observations, with percentages in parentheses. OR data are shown with 95% confidence intervals in parentheses

LI-RADS Liver Imaging Reporting and Data System, *HCC* hepatocellular carcinoma, *OR* odds ratio
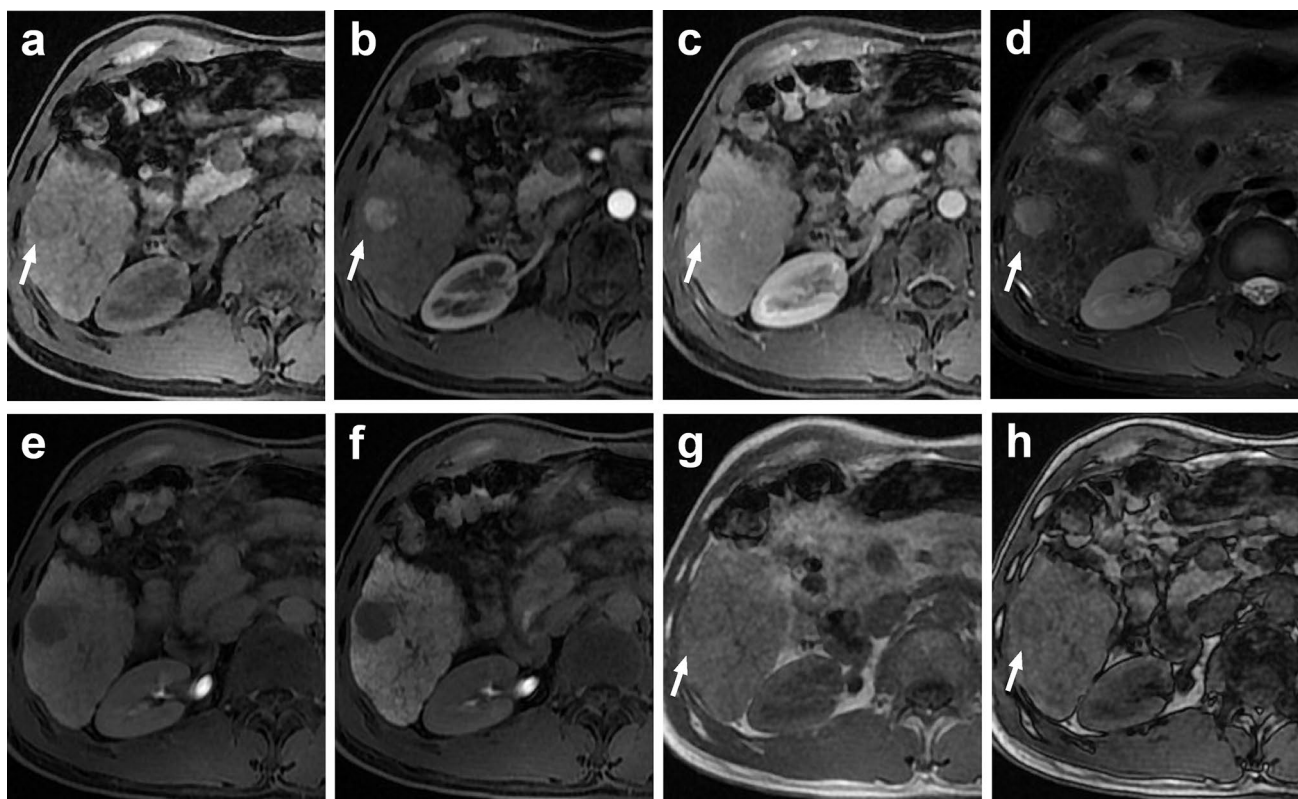
Fig. 2 Axial gadoxetic acid-enhanced MRI images from a 54-year-old man with chronic hepatitis B and surgically confirmed HCC. **a** Precontrast, **b** arterial-phase, **c** portal venous-phase, **d** T2WI FS, **e** transitional phase (TP), **f** hepatobiliary phase (HBP), **g** T1WI dual echo in-phase (IP) and **h** T1WI dual echo out-of-phase (OP) images showing an 18-mm observation in segment VI of the liver. The observation shows **a** precontrast isohypointensity (arrow), **b** nonrim arterial-phase hyperenhancement (arrow), **c** no nonperipheral washout and capsular enhancement (arrow) in the portal venous phase, **d** mild–moderate T2WI hyperintensity (arrow), **e** TP hypointensity, **f** HBP hypointensity, and slight signal loss (arrow) of OP imaging **f** compared to that of IP imaging (**e**). This hepatic observation was classified as LR-4 and could not be classified as LR-5 using Liver Imaging Reporting and Data System (LI-RADS) version 2018. In contrast, our upgraded LR-5 criteria of mLI-RADS I–III or mLI-RADS VII, utilizing independently significant ancillary features, helped achieve the correct diagnosis of HCC

55/174, 81/174, 80/174, 62/174, and 69/174, respectively (Table 3). The numbers of LR-4 in LI-RADS v2018 upgrading to LR-5 in mLI-RADS I, mLI-RADS II, and mLI-RADS III were 8/8, 7/8, and 1/8, respectively. The numbers of LR-3 in LI-RADS v2018 upgrading to LR-5 in mLI-RADS IV, mLI-RADS V, and mLI-RADS VI were 40/58, 47/58, and 10/58, respectively. The numbers of LR-4 and LR-3 in LI-RADS v2018 upgrading to LR-5 in mLI-RADS VII were 8/8 and 10/58, respectively.

The diagnostic performance of various versions for the diagnosis of 10–19 mm HCC lesions is shown in Table 3. LR-5 v2018 showed a sensitivity of 55.1% and a specificity of 98.7%. mLI-RADS I and mLI-RADS II showed higher sensitivity (62.2% vs. 55.1%, $p = 0.016$; 61.2% vs. 55.1%, $p = 0.031$, respectively) than LR-5 v2018 without compromising specificity (both 97.4% vs. 98.7%, $p > 0.999$). mLI-RADS III showed almost the same sensitivity and specificity as LR-5 v2018. mLI-RADS IV and mLI-RADS V showed higher sensitivity (82.7% vs. 55.1%, $p < 0.001$, and 81.6%

vs. 55.1%, $p < 0.001$, respectively) than LR-5 v2018 but low specificity (81.6% vs. 98.7%, $p < 0.001$, and 71.1% vs. 98.7%, $p < 0.001$, respectively). mLI-RADS VI and mLI-RADS VII showed higher sensitivity (63.3% vs. 55.1%, $p = 0.008$, and 70.4% vs. 55.1%, $p < 0.001$, respectively) than LR-5 v2018 but similarly high specificity (96.1% vs. 98.7%, $p = 0.500$, and 94.7% vs. 98.7%, $p = 0.250$, respectively).

Discussion

Our study demonstrates that three of the AFs favoring malignancy (mild–moderate T2 hyperintensity, TP hypointensity and fat in mass) were independently significant features for the noninvasive diagnosis of 10–19 mm HCC observed on gadoxetic acid-enhanced MRI. When using mild–moderate T2 hyperintensity/TP hypointensity to upgrade an observation from LR-4 to LR-5 or using fat in mass to upgrade an observation from LR-3 to LR-5, the sensitivity was
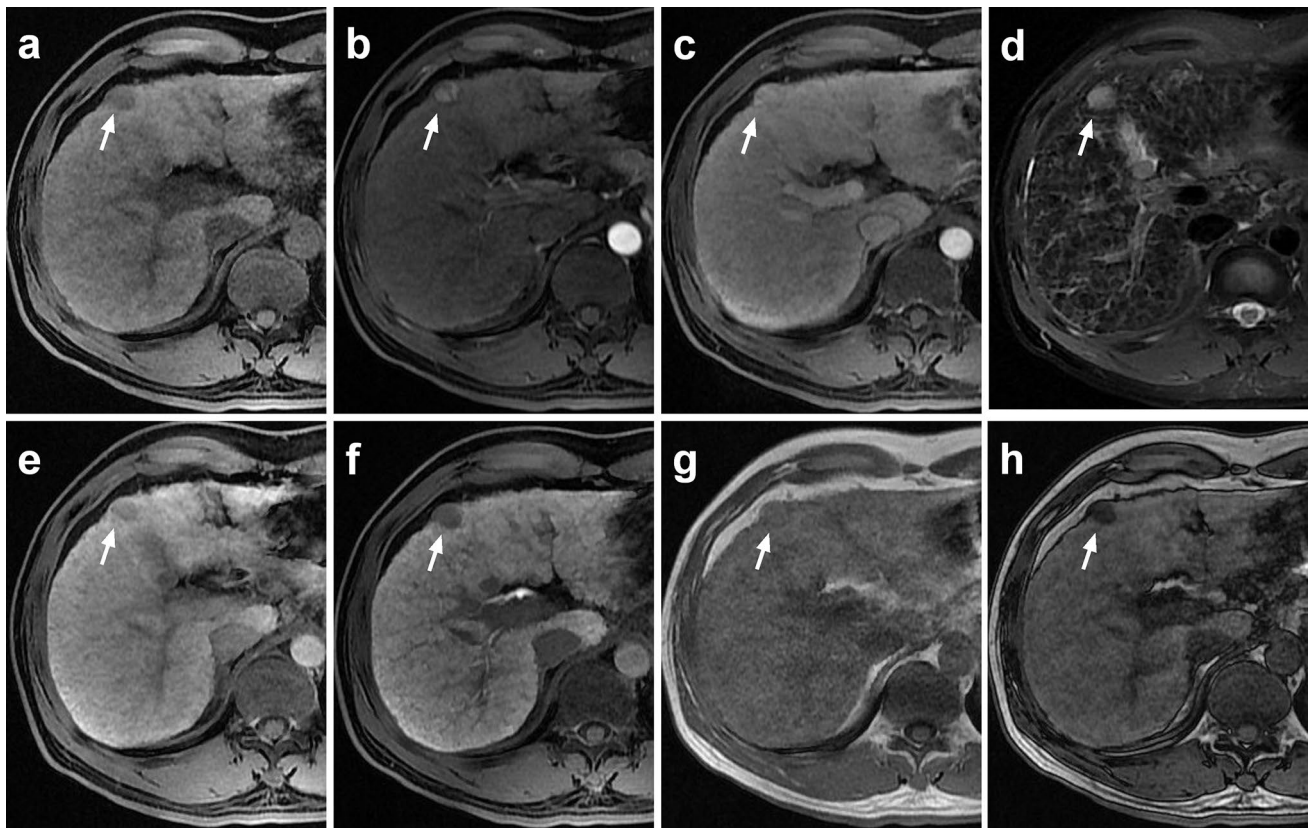
Fig. 3 Axial gadoxetic acid-enhanced MRI images from a 52-year-old man with chronic hepatitis B and surgically confirmed HCC. **a** Precontrast, **b** arterial-phase, **c** portal venous-phase, **d** T2WI FS, **e** transitional phase (TP), **f** hepatobiliary phase (HBP), **g** T1WI dual echo in-phase (IP), and **h** T1WI dual echo out-of-phase (OP) images showing a 16-mm observation in segment IV of the liver. The observation shows **a** precontrast hypointensity (arrow), **b** arterial-phase hyperenhancement (arrow), **c** no washout (arrow) in the portal venous phase, **d** mild–moderate T2WI hyperintensity (arrow), **e** TP hypointensity (arrow), **f** HBP hypointensity (arrow), and signal loss (arrow) on OP imaging (**h**) compared to that of IP imaging (**g**). This hepatic observation was classified as LR-3 and could not be classified as LR-5 using Liver Imaging Reporting and Data System (LI-RADS) version 2018. In contrast, our upgraded LR-5 criteria of mLI-RADS IV–VII, utilizing independently significant ancillary features, helped achieve the correct diagnosis of HCC

Table 3 Diagnostic performance of various versions for the diagnosis of 10–19 mm HCC lesions

Diagnostic criteria	Upgrade number	Total/final number	Sensitivity		Specificity	
			%	p value*	%	p value*
LR-5 v2018		54/174	55.1 (44.7–65.1)	–	98.7 (91.9–99.9)	–
mLI-RADS I	7	61/174	62.2 (51.8–71.7)	0.016	97.4 (90.0–99.5)	> 0.999
mLI-RADS II	6	60/174	61.2 (50.8–70.7)	0.031	97.4 (90.0–99.5)	> 0.999
mLI-RADS III	1	55/174	56.1 (45.7–66.0)	> 0.999	98.7 (91.9–99.9)	> 0.999
mLI-RADS IV	27	81/174	82.7 (73.4–89.3)	< 0.001	81.6 (70.7–89.2)	< 0.001
mLI-RADS V	26	80/174	81.6 (72.3–88.5)	< 0.001	71.1 (59.4–80.6)	< 0.001
mLI-RADS VI	8	62/174	63.3 (52.9–72.6)	0.008	96.1 (88.1–99.0)	0.500
mLI-RADS VII	15	69/174	70.4 (60.2–79.0)	< 0.001	94.7 (86.4–98.3)	0.250

Data in parentheses are 95% confidence intervals. Except for the LR-5 observations as defined by LI-RADS v2018, observations that meet the following criteria were also categorized as LR-5 in the mLI-RADS versions

HCC hepatocellular carcinoma, *LR-5 v2018* the standard LR-5 of Liver Imaging Reporting and Data System version 2018, *mLI-RADS I* LR-4 + mild–moderate T2 hyperintensity, *mLI-RADS II* LR-4 + TP hypointensity, *mLI-RADS III* LR-4 + fat in mass, *mLI-RADS IV* LR-3 + mild–moderate T2 hyperintensity, *mLI-RADS V* LR-3 + TP hypointensity, *mLI-RADS VI* LR-3 + fat in mass, *mLI-RADS VII* LR-4 + mild–moderate T2 hyperintensity/TP hypointensity or LR-3 + fat in mass

*In comparison with LR-5 v2018

significantly improved compared with that of LI-RADS v2018, while the specificity was not significantly reduced for diagnosing 10–19 mm HCC observed on gadoxetic acid-enhanced MRI.

Recent studies have shown that modified MFs, such as APHE evaluated using an arterial subtraction sequence [23, 24] or extended washout or capsule criteria on gadoxetic acid-enhanced MRI [17, 25, 26], could improve the sensitivity of LR-5 for diagnosing HCC. Previous studies have revealed that some AFs, such as hypointensity in the transitional or HBP, nonenhancing "capsule" and restricted diffusion, could improve sensitivity for the diagnosis of HCC [11, 17, 26–31]. However, few studies have assessed the role of AFs in LI-RADS using gadoxetic acid-enhanced MRI for the diagnosis of 10–19 mm HCC. Our study included all AFs of LI-RADS v2018 to determine independent features for predicting 10–19 mm HCC lesions on gadoxetic acid-enhanced MRI, and our results demonstrate that only mild–moderate T2 hyperintensity, TP hypointensity and 'fat in mass' were significant and independent features for the diagnosis of 10–19 mm HCC. This implies that mild–moderate T2 hyperintensity, TP hypointensity and 'fat in mass' may be more important than other AFs, and therefore, we try to explore the role of the independent significant AFs to upgrading LR-3/4 to LR-5.

In our study, mild–moderate T2 hyperintensity was a significant independent feature for the diagnosis of 10–19 mm HCC on gadoxetic acid-enhanced MRI. Moreover, when using mild–moderate T2 hyperintensity to upgrade an observation from LR-4 to LR-5, the sensitivity was significantly improved (from 55.1 to 62.2%) without impairing specificity (from 98.7% to 97.4%) for diagnosing 10–19 mm HCC on gadoxetic acid-enhanced MRI. Previous studies have reported that mild–moderate T2 hyperintensity is an important feature for the early detection of HCC or predicting the malignant transformation of hypovascular nodules [31–34]. Our study is consistent with these studies. In terms of pathological changes, T2 hyperintensity may reflect intratumoral sinusoid dilation and edema. T2WI signals correlate with intranodular arterial flow and inversely with intranodular portal venous flow, pathophysiological alterations associated with hepatocarcinogenesis [32]. In addition, 83–86% of all HCCs have T2 hyperintensity [35]. Additionally, using mild–moderate T2 hyperintensity to upgrade an observation from LR-3 to LR-5 provided the highest sensitivity (82.7%) for the diagnosis of 10–19 mm HCC, but with reduced specificity (81.6% vs. 98.7%, $p < 0.001$). The reason for this result may be the higher proportion of non-HCC LR-3 lesions with mild–moderate T2 hyperintensity in our study (13/25, 52.0%). In our study, while mild–moderate T2 hyperintensity was highly suggestive of malignancy, it was also seen in non-HCC malignancies [35]. Thus, the presence of mild–moderate T2 hyperintensity alone may not be used to establish a diagnosis of HCC in the absence of MFs.

TP hypointensity was also a significant independent feature for the diagnosis of 10–19 mm HCC lesions on gadoxetic acid-enhanced MRI. Our study results are in good agreement with the results of a previous study by Choi et al. [30], which demonstrated that TP hypointensity is an independent predictor of HCC in lesions ≤ 3 cm with gadoxetic acid-enhanced dynamic MRI. Furthermore, our results showed that when using TP hypointensity to upgrade an observation from LR-4 to LR-5, the sensitivity was higher (55.1% vs. 61.2%, $p = 0.031$) while maintaining sufficiently specificity (98.7% vs. 97.4%, $p < 0.05$) than compared to that of LI-RADS v2018 for diagnosing 10–19 mm HCC on gadoxetic acid-enhanced MRI. This may be due to the portal supply and organic anion transporter (OATP) expression usually diminishing during hepatocarcinogenesis [36], resulting in TP hypointensity in gadoxetic acid-enhanced MRI. However, when using TP hypointensity to upgrade an observation from LR-3 to LR-5, the sensitivity was improved, and the specificity was significantly impaired. The reason for this result may be the higher proportion of non-HCC LR-3 lesions with TP hypointensity (21/47, 44.6%) and all of these lesions were benign lesions in our study. Further study with a larger sample size is warranted to validate our results.

Fat in mass is another significant independent feature for the diagnosis of small HCC with gadoxetic acid-enhanced MRI. Recent studies have revealed that the MRI of detection of intralesional fat in patients at high risk for HCC on MRI favors the diagnosis of HCC [37–39]. Previous research has shown that up to 40% of early HCCs exhibit fat in histology [40]. Furthermore, Kutami et al. found that fatty changes in small HCC lesions are closely related to tumor size [40]. Intralesional fat is most frequent in small HCCs, and the frequency decreases with increasing size. Importantly, fat in mass is extremely rare in non-HCC hepatic malignancies; thus, the detection of fat may help to exclude ICC in problematic cases [39]. The presence of intralesional fat has been considered a marker of carcinogenesis from dysplasia to HCC in CT or MRI [41, 42]. This feature is attributable to a decrease in intratumoral arteries without alterations of intratumoural portal tracts [40]. This may explain why fat in mass could upgrade an observation from LR-3 to LR-5 with higher sensitivity without significantly reducing the specificity compared with that of LI-RADS v2018 for diagnosing 10–19 mm HCC with gadoxetic acid-enhanced MRI. However, when using fat in mass to upgrade an observation from LR-4 to LR-5, the sensitivity and specificity remained nearly the same as those of the original LI-RADS v2018. This may be because that only one LR-4 lesion in this study showed 'fat in mass'. This may explain why 'fat in mass' did not contribute to the upgrading of lesions from LR-4 to

LR-5. Further research with a larger number of LR-4 lesions is warranted to validate our findings.

HBP hypointensity has previously been reported as an independently significant feature for the diagnosis of HCC [11, 43, 44]. In particular, in a recent similar study performed by Lee et al. [31], four AFs (mild–moderate T2 hyperintensity, HBP hypointensity, nonenhancing "capsule" and mosaic architecture) were independently significant features, along with all the MFs. The results of these studies are different from those of our study. This may be because the number of cases, etiology and observation size (10–19 mm) in our study were different from those in the other studies. Another reason may be that HBP hypointensity showed relatively low specificity (25%) in our study.

There are several limitations to our study. First, this was a single-center retrospective study, which may have selection bias. Multicentric prospective studies are warranted to validate our results. Second, most of the patients included in this study had compensated liver function, and most patients had hepatitis B infection. The results of this study might not be directly adapted to, for example, Western populations with a higher expected proportion of patients with decompensated liver function and different underlying chronic liver diseases (hepatitis C, alcoholic steatohepatitis, nonalcoholic steatohepatitis, etc.). Third, the proportion of males was higher than that of females in our study. That may be due to HBV infection is mostly in males in China and our study was based on 10–19 mm observations, which may have selection bias. Fourth, the number of LR-4 lesions included in the study was relatively small. Further work using a population with larger LR-4 lesions is needed to confirm the value of AFs for diagnosing 10–19 mm HCC lesions on gadoxetic acid-enhanced MRI. Finally, we used a composite reference standard for the determination of benignity. However, biopsy is not always performed in the clinic for highly suspected benign lesions, and the application of a strict reference (e.g., pathology) for benign observations may lead to additional selection bias. Patients with observations without pathological results were followed up for at least 2 years to make a final diagnosis, which better represents clinical practice.

In conclusion, our results show that upgrading an observation from LR-3/LR-4 to LR-5 using independently significant AFs (mild–moderate T2 hyperintensity, TP hypointensity or fat in mass) can improve sensitivity without impairing specificity in the diagnosis of 10–19 mm HCC lesions on gadoxetic acid-enhanced MRI.

Declarations

References

1. Villanueva A (2019) Hepatocellular Carcinoma. N Engl J Med 380(15):1450–1462. https://doi.org/10.1056/NEJMra1713263

2. Ronot M, Fouque O, Esvan M, Lebigot J, Aubé C, Vilgrain V (2018) Comparison of the accuracy of AASLD and LI-RADS criteria for the non-invasive diagnosis of HCC smaller than 3 cm. J Hepatol 68(4):715–723. https://doi.org/10.1016/j.jhep.2017.12.014

3. Heimbach JK, Kulik LM, Finn RS, et al (2018) AASLD guidelines for the treatment of hepatocellular carcinoma. Hepatology 67(1):358–380. https://doi.org/10.1002/hep.29086

4. European Association for the Study of the Liver (2018) EASL Clinical Practice Guidelines: Management of hepatocellular carcinoma. J Hepatol 69(1):182–236. https://doi.org/10.1016/j.jhep.2018.03.019

5. Xie DY, Ren ZG, Zhou J, Fan J, Gao Q (2017) Critical appraisal of Chinese 2017 guideline on the management of hepatocellular carcinoma. Hepatobiliary Surg Nutr 6(6):387–396. https://doi.org/10.21037/hbsn.2017.11.01

6. Santillan C, Chernyak V, Sirlin C (2018) LI-RADS categories: concepts, definitions, and criteria. Abdom Radiol (NY) 43(1):101–110. https://doi.org/10.1007/s00261-017-1334-x

7. Kim BR, Lee JM, Lee DH, et al (2017) Diagnostic Performance of Gadoxetic Acid-enhanced Liver MR Imaging versus Multidetector CT in the Detection of Dysplastic Nodules and Early Hepatocellular Carcinoma. Radiology 285(1):134–146. https://doi.org/10.1148/radiol.2017162080

8. Shah A, Tang A, Santillan C, Sirlin C (2016) Cirrhotic liver: What's that nodule? The LI-RADS approach. J Magn Reson Imaging 43(2):281–294. https://doi.org/10.1002/jmri.24937

9. Lee SM, Lee JM, Ahn SJ, Kang HJ, Yang HK, Yoon JH (2019) LI-RADS Version 2017 versus Version 2018: Diagnosis of Hepatocellular Carcinoma on Gadoxetate Disodium-enhanced MRI. Radiology 292(3):655–663. https://doi.org/10.1148/radiol.2019182867

10. Roberts LR, Sirlin CB, Zaiem F, et al. (2018) Imaging for the diagnosis of hepatocellular carcinoma: A systematic review and meta-analysis. Hepatology 67(1):401–421. https://doi.org/10.1002/hep.29487

11. Renzulli M, Biselli M, Brocchi S, et al (2018) New hallmark of hepatocellular carcinoma, early hepatocellular carcinoma and high-grade dysplastic nodules on Gd-EOB-DTPA MRI in patients with cirrhosis: a new diagnostic algorithm. GUT 67(9):1674–1682. https://doi.org/10.1136/gutjnl-2017-315384

12. Choi SH, Lee SS, Park SH, et al (2019) LI-RADS Classification and Prognosis of Primary Liver Cancers at Gadoxetic Acid-enhanced MRI. Radiology 290(2):388–397. https://doi.org/10.1148/radiol.2018181290

13. Golfieri R, Grazioli L, Orlando E, et al (2012) Which is the best MRI marker of malignancy for atypical cirrhotic nodules: hypointensity in hepatobiliary phase alone or combined with other features? Classification after Gd-EOB-DTPA administration. J Magn Reson Imaging 36(3):648–657. https://doi.org/10.1002/jmri.23685

14. Granito A, Galassi M, Piscaglia F, et al (2013) Impact of gadoxetic acid (Gd-EOB-DTPA)-enhanced magnetic resonance on the non-invasive diagnosis of small hepatocellular carcinoma: a prospective study. Aliment Pharmacol Ther 37(3):355–363. https://doi.org/10.1111/apt.12166

15. Joo I, Lee JM, Lee DH, Jeon JH, Han JK, Choi BI (2015) Noninvasive diagnosis of hepatocellular carcinoma on gadoxetic acid-enhanced MRI: can hypointensity on the hepatobiliary phase be used as an alternative to washout? Eur Radiol 25(10):2859–2868. https://doi.org/10.1007/s00330-015-3686-3

16. Kwon HJ, Byun JH, Kim JY, et al (2015) Differentiation of small (≤2 cm) hepatocellular carcinomas from small benign nodules in cirrhotic liver on gadoxetic acid-enhanced and diffusion-weighted magnetic resonance images. Abdom Imaging 40(1):64–75. https://doi.org/10.1007/s00261-014-0188-8

17. Joo I, Lee JM, Lee DH, Jeon JH, Han JK (2019) Retrospective validation of a new diagnostic criterion for hepatocellular carcinoma on gadoxetic acid-enhanced MRI: can hypointensity on the hepatobiliary phase be used as an alternative to washout with the aid of ancillary features? Eur Radiol 29(4):1724–1732. https://doi.org/10.1007/s00330-018-5727-1

18. Min JH, Kim JM, Kim YK, et al (2018) Prospective Intraindividual Comparison of Magnetic Resonance Imaging with Gadoxetic Acid and Extracellular Contrast for Diagnosis of Hepatocellular Carcinomas Using the Liver Imaging Reporting and Data System. Hepatology 68(6):2254–2266. https://doi.org/10.1002/hep.30122

19. Cha DI, Jang KM, Kim SH, Kang TW, Song KD (2017) Liver Imaging Reporting and Data System on CT and gadoxetic acid-enhanced MRI with diffusion-weighted imaging. Eur Radiol 27(10):4394–4405. https://doi.org/10.1007/s00330-017-4804-1

20. American College of Radiology. Liver imaging reporting and data system version 2018. https://www.acr.org/Clinical-Resources/Reporting-and-Data-Systems/LI-RADS/CT-MRI-LI-RADS-v2018. Accessed June 2019

21. Kleihues P, Sobin LH (2000) World Health Organization classification of tumors. Cancer 88(12):2887. https://doi.org/10.1002/1097-0142(20000615)88:12<2887::aid-cncr32>3.0.co;2-f

22. Petitclerc L, Sebastiani G, Gilbert G, Cloutier G, Tang A (2017) Liver fibrosis: Review of current imaging and MRI quantification techniques. J Magn Reson Imaging 45(5):1276–1295. https://doi.org/10.1002/jmri.25550

23. Kim DH, Choi SH, Byun JH, et al (2019) Arterial subtraction images of gadoxetate-enhanced MRI improve diagnosis of early-stage hepatocellular carcinoma. J Hepatol 71(3):534–542. https://doi.org/10.1016/j.jhep.2019.05.005

24. Choi SH, Kim SY, Lee SS, et al (2017) Subtraction Images of Gadoxetic Acid-Enhanced MRI: Effect on the Diagnostic Performance for Focal Hepatic Lesions in Patients at Risk for Hepatocellular Carcinoma. AJR Am J Roentgenol 209(3):584–591. https://doi.org/10.2214/AJR.16.17211

25. Kim DH, Choi SH, Kim SY, Kim MJ, Lee SS, Byun JH (2019) Gadoxetic Acid-enhanced MRI of Hepatocellular Carcinoma: Value of Washout in Transitional and Hepatobiliary Phases. Radiology 291(3):651–657. https://doi.org/10.1148/radiol.2019182587

26. Hwang SH, Park S, Han K, Choi JY, Park YN, Park MS (2019) Optimal lexicon of gadoxetic acid-enhanced magnetic resonance imaging for the diagnosis of hepatocellular carcinoma modified from LI-RADS. Abdom Radiol (NY) 44(9):3078–3088. https://doi.org/10.1007/s00261-019-02077-1

27. Kim DH, Choi SH, Kim SY, Kim MJ, Lee SS, Byun JH (2019) Gadoxetic Acid-enhanced MRI of Hepatocellular Carcinoma: Value of Washout in Transitional and Hepatobiliary Phases. Radiology 292(1):270. https://doi.org/10.1148/radiol.2019182587

28. Vernuccio F, Cannella R, Meyer M, et al (2019) LI-RADS: Diagnostic Performance of Hepatobiliary Phase Hypointensity and Major Imaging Features of LR-3 and LR-4 Lesions Measuring 10-19 mm With Arterial Phase Hyperenhancement. AJR Am J Roentgenol 213(2):W57–W65. https://doi.org/10.2214/AJR.18.20979

29. Rimola J, Forner A, Tremosini S, et al (2012) Non-invasive diagnosis of hepatocellular carcinoma ≤ 2 cm in cirrhosis. Diagnostic accuracy assessing fat, capsule and signal intensity at dynamic MRI. J Hepatol 56(6):1317–1323. https://doi.org/10.1016/j.jhep.2012.01.004

30. Choi SH, Byun JH, Lim YS, et al (2016) Diagnostic criteria for hepatocellular carcinoma ≤3 cm with hepatocyte-specific contrast-enhanced magnetic resonance imaging. J Hepatol 64(5):1099–1107. https://doi.org/10.1016/j.jhep.2016.01.018

31. Lee S, Kim SS, Bae H, Shin J, Yoon JK, Kim MJ (2021) Application of Liver Imaging Reporting and Data System version 2018 ancillary features to upgrade from LR-4 to LR-5 on gadoxetic acid-enhanced MRI. Eur Radiol 31(2):855–863. https://doi.org/10.1007/s00330-020-07146-4

32. Hyodo T, Murakami T, Imai Y, et al. (2013) Hypovascular nodules in patients with chronic liver disease: risk factors for development of hypervascular hepatocellular carcinoma. Radiology 266(2):480–490. https://doi.org/10.1148/radiol.12112677

33. Rhee H, Kim MJ, Park YN, Choi JS, Kim KS (2012) Gadoxetic acid-enhanced MRI findings of early hepatocellular carcinoma as defined by new histologic criteria. J Magn Reson Imaging 35(2):393–398. https://doi.org/10.1002/jmri.22828

34. Jha RC, Zanello PA, Nguyen XM, et al (2014) Small hepatocellular carcinoma: MRI findings for predicting tumor growth rates. Acad Radiol 21(11):1455–64. https://doi.org/10.1016/j.acra.2014.06.011

35. Choi JY, Lee JM, Sirlin CB (2014) CT and MR imaging diagnosis and staging of hepatocellular carcinoma: part II. Extracellular agents, hepatobiliary agents, and ancillary imaging features. Radiology 273(1):30–50. https://doi.org/10.1148/radiol.14132362

36. Choi JY, Lee JM, Sirlin CB (2014). CT and MR imaging diagnosis and staging of hepatocellular carcinoma: part I. Development, growth, and spread: key pathologic and imaging aspects. Radiology 272(3):635–654. https://doi.org/10.1148/radiol.14132361

37. Joishi D, Ueno A, Tanimoto A, Okuda S, et al (2013) Natural Course of Hypovascular Nodules Detected on Gadoxetic Acid-enhanced MR Imaging: Presence of Fat is a Risk Factor for Hypervascularization. Magn Reson Med Sci 12(4):281–287. https://doi.org/10.2463/mrms.2012-0097

38. Cho E, Choi J (2015) MRI features of hepatocellular carcinoma related to biologic behavior. Korean J Radiol 16(3):449–464.

39. You MW, Yun SJ (2019) Differentiating between hepatocellular carcinoma and intrahepatic cholangiocarcinoma using contrast-enhanced MRI features: a systematic review and meta-analysis. Clin Radiol 74(5):406.e9–406.e18. https://doi.org/10.3348/kjr.2015.16.3.449

40. Kutami R, Nakashima Y, Nakashima O, Shiota K, Kojiro M (2000) Pathomorphologic study on the mechanism of fatty change in small hepatocellular carcinoma of humans. J Hepatol 33(2):282–-289. https://doi.org/10.1016/s0168-8278(00)80369-4

41. Yu JS, Chung JJ, Kim JH, Kim KW (2007) Fat-containing nodules in the cirrhotic liver: chemical shift MRI features and clinical implications. AJR Am J Roentgenol 188(4):1009–1016. https://doi.org/10.2214/AJR.06.0756

42. Martin J, Sentis M, Zidan A, et al (1995) Fatty metamorphosis of hepatocellular carcinoma: detection with chemical shift gradient-echo MR imaging. Radiology 195(1):125–130. https://doi.org/10.1148/radiology.195.1.7892452

43. Cannella R, Vernuccio F, Sagreiya H, et al (2020) Liver Imaging Reporting and Data System (LI-RADS) v2018: diagnostic value of ancillary features favoring malignancy in hypervascular observations ≥ 10 mm at intermediate (LR-3) and high probability (LR-4) for hepatocellular carcinoma. Eur Radiol 30(7):3770–3781. https://doi.org/10.1007/s00330-020-06698-9

44. Kang JH, Choi SH, Byun JH, et al (2020) Ancillary features in the Liver Imaging Reporting and Data System: how to improve diagnosis of hepatocellular carcinoma ≤ 3 cm on magnetic resonance imaging. Eur Radiol 30(5):2881–2889. https://doi.org/10.1007/s00330-019-06645-3